MOLECULAR AND CELLULAR BIOLOGY, Aug. 1987, p. 2753–2761
0270-7306/87/082753-09$02.00/0

Vol. 7, No. 8

Transcription of the Constitutively Expressed Yeast Enolase Gene *ENO1* Is Mediated by Positive and Negative *cis*-Acting Regulatory Sequences

REGINA COHEN, TERESA YOKOI, JANICE P. HOLLAND, ALAN E. PEPPER, AND MICHAEL J. HOLLAND*

Department of Biological Chemistry, School of Medicine, University of California, Davis, California 95616

Received 20 June 1986/Accepted 8 May 1987

There are two enolase genes, *ENO1* and *ENO2*, per haploid yeast genome. Expression of the *ENO1* gene is quantitatively similar in cells grown on glucose or gluconeogenic carbon sources. In contrast, *ENO2* expression is induced more than 20-fold in cells grown on glucose as the carbon source. *cis*-Acting regulatory sequences were mapped within the 5′-flanking region of the constitutively expressed yeast enolase gene *ENO1*. A complex positive regulatory region was located 445 base pairs (bp) upstream from the transcriptional initiation site which was required for *ENO1* expression in cells grown on glycolytic or gluconeogenic carbon sources. A negative regulatory region was located 160 bp upstream from the transcriptional initiation site. Sequences required for the function of this negative regulatory element were mapped to a 38-bp region. Deletion of all or a portion of these latter sequences permitted glucose-dependent induction of *ENO1* expression that was quantitatively similar to that of the glucose-inducible *ENO2* gene. The negative regulatory element therefore prevents glucose-dependent induction of the *ENO1* gene. Hybrid 5′-flanking regions were constructed which contained the upstream regulatory sequences of one enolase gene fused at a site upstream from the TATAAA box in the other enolase gene. Analysis of the expression of enolase genes containing these hybrid 5′-flanking region showed that the positive regulatory regions of *ENO1* and *ENO2* were functionally similar, as were the regions extending from the TATAAA boxes to the initiation codons. Based on these studies, we conclude that the negative regulatory element plays the critical role in maintaining the constitutive expression of the *ENO1* structural gene in cells grown on glucose or gluconeogenic carbon sources.

Enolase is one of the most abundant enzymes in *Saccharomyces cerevisiae*. There are two yeast enolase structural genes, designated *ENO1* and *ENO2*, which encode polypeptides differing in 20 of 436 amino acid residues (3). The two genes are expressed differentially in vegetative cells grown on glycolytic or gluconeogenic carbon sources. The steady-state concentrations of the *ENO1*-encoded mRNA and polypeptide are similar in cells grown on the two carbon sources, whereas the intracellular concentrations of the *ENO2*-encoded mRNA and polypeptide are more than 20-fold higher in cells grown on glucose than on glycerol plus lactate (9). We showed previously that transcription of the *ENO2* gene is regulated by upstream activation sequences located approximately 460 base pairs (bp) upstream from the transcription initiation site (2). Genetic analysis further showed that sequences within this regulatory region mediate the observed glucose-dependent induction of transcription of *ENO2* (2).

Having located the *cis*-acting sequences which regulate transcription of the *ENO2* structural gene, we were interested to determine how transcription of the constitutively expressed *ENO1* structural gene is regulated. Of particular interest is the issue of coordinate regulation of transcription of the two genes. Clifton et al. (1) showed that the specific activity of enolase and other glycolytic genes is reduced approximately 50-fold in cells carrying the recessive *gcr1-1* mutation. We have shown that the *gcr1-1* mutation causes a 20- to 50-fold reduction in transcription of both enolase genes as well as the glyceraldehyde-3-phosphate dehydrogenase gene family (4). Based on these observations, it is clear that transcription of the enolase gene is coordinately regulated. It is therefore possible that *cis*-acting regulatory regions of the two enolase genes have structural or functional similarities.

In this report, we define the locations of *cis*-acting sequences which are involved in regulating transcription of the *ENO1* structural gene. Positive regulatory sequences which are required for *ENO1* gene expression are located approximately 445 bp upstream from the transcription initiation site. This regulatory region is functionally similar to the upstream regulatory region in *ENO2* and is capable of mediating glucose-dependent induction of transcription. Evidence is presented that a second regulatory region, located 162 bp upstream from the transcriptional initiation site, interferes with glucose-dependent induction of transcription of *ENO1*, resulting in the observed constitutive expression of the wild-type gene in cells grown on glucose or glycerol plus lactate.

MATERIALS AND METHODS

Materials. *Sal*I restriction endonuclease linkers were purchased from Collaborative Research, Inc. Oligonucleotide primers for sequencing deletion mutants were generously provided by Corey Levinson, Cetus Corp. ^{125}I-protein A was generously provided by John Hershey, University of California, Davis.

Strains and growth conditions. *S. cerevisiae* S173-6B (α *leu2-3 leu2-112 his3-Δ1 trp1-289 ura3-52*) was provided by F. Sherman, University of Rochester. *S. cerevisiae* S173-LA (α *leu2-3 leu2-112 his3-Δ1 trp1-289 ura3-52 eno1-1*) was con-

* Corresponding author.

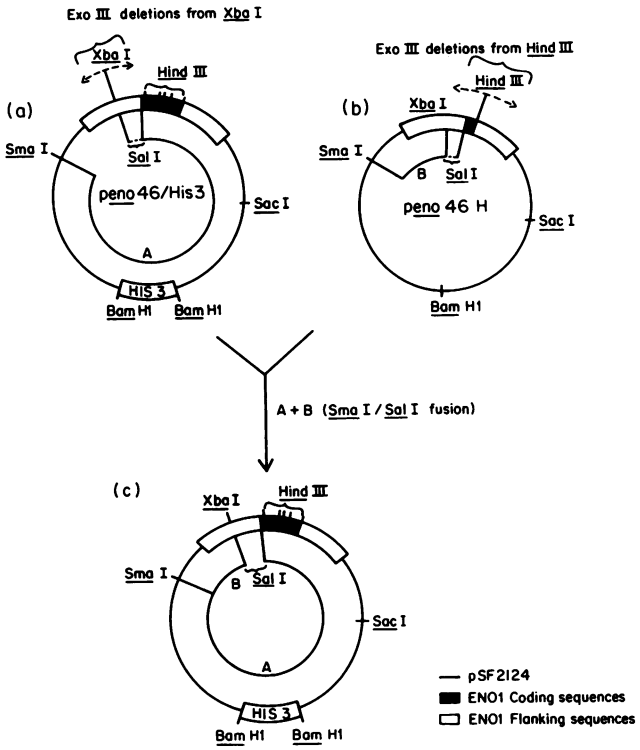

FIG. 1. Construction of deletions and *Sal*I insertion mutations within the 5'-flanking sequences of the *ENO1* gene. (a) Plasmid peno46/HIS3 contains the *ENO1* gene and a yeast *HIS3* gene on the plasmid vector pSF2124. (b) Plasmid peno46H was generated from plasmid peno46/HIS3 by joining the distal *Hin*dIII sites in the *ENO1* coding sequences and removing the *Bam*HI fragment containing the yeast *HIS3* gene. Deletions were generated from the unique *Xba*I site in peno46/HIS3 and from the unique *Hin*dIII site in peno46H by exonuclease III (Exo III) and S1 nuclease digestion as described in Materials and Methods. The exonuclease III- and S1 nuclease-treated plasmid DNA was ligated in the presence of *Sal*I linkers to generate a unique *Sal*I site at each deletion endpoint. (c) Plasmids containing the deletion and *Sal*I insertion mutation within the 5'-flanking region of the *ENO1* gene were constructed by ligating DNA fragments A, originated from the deletion mutation constructed in peno46/HIS3, to DNA fragments B, originated from the deletion mutations constructed in peno46H. The endpoints of the deletion mutations in plasmids peno46/HIS3 and peno46H were determined by the dideoxy sequencing method (11) with several oligonucleotide primers complementary to the sequences within the *ENO1* 5'-flanking region.

structed from strain S173-6B and carries a deletion of 90% of the *ENO1* coding sequences (9). Yeast strains were grown at 30°C in YP medium (1% yeast extract, 2% peptone) or in a defined medium containing 0.67% yeast nitrogen base without amino acids (Difco Laboratories) supplemented with 2 μg each of uracil, leucine, and tryptophan per ml. Histidine (2 μg/ml) was included in the medium for strains lacking a functional *HIS3* gene. Carbon sources were 2% glucose or 2% glycerol plus 2% lactate.

Construction of deletion and insertion mutations within the 5'-flanking region of the *ENO1* structural gene. Deletion and insertion mutations were constructed in the 5'-flanking region of *ENO1* by using the linker scanner method of McKnight and Kingsbury (10). The strategy for constructing these mutants was similar to the approach used to construct deletion and insertion mutations in the 5'-flanking region of *ENO2* (2). All of the mutations were generated in a region of *ENO1* extending from an *Xba*I cleavage site located at position −767 relative to the transcription initiation site. The overall strategy for isolating these deletion and insertion mutants is outlined in Fig. 1. Plasmid peno46/HIS3 contains a 4.6-kilobase (kb) segment of yeast genomic DNA which includes the entire *ENO1* structural gene ligated by the A/T tailing method at the *Eco*RI site of the vector pSF2124 (9). This plasmid also contains a functional yeast *HIS3* gene on a 1.7-kb fragment ligated at the *Bam*HI site of pSF2124. The first series of deletion mutations was generated from the unique *Xba*I site (Fig. 1a) by using exonuclease III and S1 nuclease as described previously (2). Linear plasmid DNA was ligated in the presence of a 20-fold molar excess of phosphorylated *Sal*I linker molecules to create a unique *Sal*I cleavage site and an 8-bp insertion at the endpoint of each deletion mutation. A second collection of deletion and insertion mutations was constructed by using the plasmid peno46H. This latter plasmid was derived from plasmid peno46 by removal of four *Hin*dIII fragments from within the coding sequences of *ENO1* as described previously (9). Deletion mutations were generated from the unique *Hin*dIII site at codon 45 in the *ENO1* coding sequences as described above (Fig. 1b). A *Sal*I linker molecule was inserted at the endpoint of each deletion mutation. Following transformation of competent *Escherichia coli* with ligated DNA derived from each collection of deletion and insertion mutations, plasmid DNA was isolated from cloned transformants and analyzed by restriction endonuclease digestion to determine the approximate size of the deletion in each isolated plasmid. The exact endpoints of the deletion mutations in representative plasmids were determined by DNA sequence analysis.

The final construction of deletion and insertion mutations in the 5'-flanking region of *ENO1* is outlined in Fig. 1c. A DNA fragment extending downstream from the *Sal*I site to the *Sma*I site in the vector was isolated from a plasmid derived from the second collection of deletion mutants (fragment B, Fig. 1b). Approximately equimolar amounts of the two DNA fragments were ligated and used to transform competent *E. coli*. By isolating the two *Sma*I-*Sal*I fragments from plasmids containing deletion mutations of known size, it was possible to generate a deletion or insertion mutation of known dimensions at any position within the 5'-flanking sequences of *ENO1*. The final *Sma*I-*Sal*I fusion step also restored the *HIS3* gene in the vector. This strategy was used to construct deletions extending from position −767 toward the translational initiation codon by using an *Sma*I-*Sal*I fragment (fragment B) isolated from peno46/His3, in which the *Sal*I linker was inserted at the *Xba*I site.

Analysis of expression of mutant *ENO1* genes. *S. cerevisiae* S173-LA was transformed to histidine prototrophy by the procedure of Ito et al. (6) with plasmids containing the deletion and insertion mutations described in the preceding section. Supercoiled plasmids or plasmids linearized with *Xba*I were used in the transformation. In each case, expression of the mutant *ENO1* gene was analyzed in at least three independent transformants. Total cell protein was extracted from cells grown to early log phase by vortexing in the presence of glass beads as described previously (2). Western blotting (immunoblotting) analysis was carried out after one-dimensional sodium dodecyl sulfate (SDS)-polyacrylamide gel electrophoresis with a rabbit polyclonal antibody which cross-reacts with the enolase 1 and enolase 2 polypeptides (2, 9). The steady-state concentration of the enolase 1 polypeptide was measured relative to the enolase 2 poly-

peptide encoded by the resident *ENO2* structural gene. Quantitation of the amount of enolase 1 polypeptide relative to enolase 2 polypeptide was carried out by the method of Howe and Hershey (5). Sections of the ^{125}I-labeled immunoblot corresponding to the enolase 1 and 2 polypeptides as well as sections representative of the background were sliced, and the amount of ^{125}I in each section was determined with a Tracor 1197 gamma counter.

Southern blotting analysis was carried out with genomic DNA isolated from at least one transformant obtained after transformation with plasmids carrying each deletion and insertion mutation as described previously (2). This analysis confirmed that the entire plasmid was recombined at the *ENO1* locus of the recipient strain. As in the case of integration of hybrid *ENO2-ENO1* genes at the *ENO1* locus (2), the orientation of the incoming mutant gene relative to the resident *eno1* deletion was always such that normal *ENO1* chromosomal sequences were 5′ to the mutation. In the case of transformations with supercoiled plasmids, we assume that this preferred orientation of integration is due to the presence of an efficient recombination site upstream from the *Xba*I site in peno46/His3.

The intracellular concentration of *ENO1* mRNA was determined by Northern blotting analysis as described previously (2). A hybridization probe complementary to the 3′ untranslated portion of *ENO1* mRNA was used for this analysis. This probe was prepared by nick-translation of a 1.4-kb *Hin*dIII-*Eco*RI fragment of DNA isolated from plasmid peno46 (2, 3).

Construction of *ENO1-ENO2* and *ENO2-ENO1* gene fusions. Fusions between the 5′-flanking sequences of *ENO2* and *ENO1* were constructed by ligating segments of the 5′-flanking region of one enolase gene at sites upstream from the TATAAA box in the second enolase gene. Genes containing *ENO1-ENO2* hybrid 5′-flanking regions were constructed in the following manner. A plasmid, designated penoF1, was constructed as previously described (2). This plasmid was derived from plasmid peno46/HIS3 by replacing *ENO1* sequences extending from the *Xba*I site at position −767 to the *Hin*dIII site at codon 45 with *ENO2* sequences extending from an *Xba*I site at position −1300 to a homologous *Hin*dIII site at codon 45. We showed previously (2) that this gene fusion encodes the enolase 1 polypeptide and that regulation of expression of this gene fusion is quantitatively the same as the *ENO2* gene. A penoF1 plasmid containing a *Sal*I linker insertion at position −229 was constructed as described previously (2). *ENO2* sequences in this latter plasmid extending from the *Xba*I site at position −1300 to the *Sal*I site at position −229 were replaced with *ENO1* sequences extending from the *Xba*I site at position −767 variable distances toward position −121.

Genes containing *ENO2-ENO1* hybrid 5′-flanking regions were constructed by the following procedure. Plasmid peno46/HIS3, containing a *Sal*I linker insertion at position −121, was constructed as described above. *ENO1* sequences in this plasmid, extending from the *Xba*I site at position −767 to the *Sal*I site at position −121, were replaced with *ENO2* 5′-flanking sequences extending from an *Xba*I site at position −1300 variable distances toward position −190.

Expression of both series of genes containing hybrid 5′-flanking sequences was monitored by Western blotting of whole-cell extracts isolated from transformants carrying each hybrid gene integrated at the *ENO1* locus of the *eno1* recipient yeast strain S173-LA.

DNA sequencing. The DNA sequence of the *ENO1* 5′-flanking region between the *Xba*I site at position −767 and the translation initiation codon was determined on both strands by the method of Maxam and Gilbert (8). Routine identification of the endpoints of deletion and insertion mutations within the 5′-flanking region of *ENO1* was determined by the dideoxy sequencing method (11) with several synthetic oligonucleotide primers complementary to sequences on each strand of the *ENO1* 5′-flanking region.

RESULTS

Mapping of the 5′ and 3′ boundaries of the *cis*-acting regulatory sequences within the 5′-flanking region of *ENO1*. To locate *cis*-acting sequences which regulate expression of the *ENO1* structural gene, plasmids carrying deletion mutations within the 5′-flanking region of the cloned gene were constructed as described in Materials and Methods (Fig. 1). Previous studies with an *ENO2-ENO1* gene fusion in which *ENO1* 5′-flanking sequences extending from an *Xba*I cleavage site at position −767 to the translation initiation codon were replaced with the 5′-flanking region of the *ENO2* structural gene suggest that *cis*-acting sequences which regulate *ENO1* expression reside between the *Xba*I site and the initiation codon. The nucleotide sequence of this region is shown in Fig. 2. Plasmids containing deletion and insertion mutations within the *ENO1* 5′-flanking region and a selectable yeast *HIS3* structural gene were used to transform a recipient strain (*eno1 his3*) carrying a deletion of 90% of the coding sequences of the resident *ENO1* gene. Expression of each mutant *ENO1* gene was monitored in at least three independent transformants by Western blotting following one-dimensional SDS-polyacrylamide gel electrophoresis of whole-cell extracts prepared from early-log-phase cultures. The steady-state concentration of the enolase 1 polypeptide was determined relative to the concentration of the enolase 2 polypeptide encoded by the resident *ENO2* gene. Southern blotting analysis was carried out on genomic DNA isolated from at least one transformant to confirm that the entire plasmid was integrated at the *ENO1* locus of the recipient strain and that the orientation of the integration was such that normal *ENO1* chromosomal sequences flanked the mutant *ENO1* gene being analyzed.

To map the apparent 5′ boundaries of *cis*-acting regulatory sequences, a series of deletion and insertion mutations were analyzed which extended from the *Xba*I site at position −767 variable distances toward the translation initiation codon. The coordinates of these mutations are illustrated in Fig. 3. The Western blotting analyses for representative mutants are shown in Fig. 4. Expression of *ENO1* genes carrying deletion mutations extending from position −767 to position −447 was similar to the wild-type gene in cells grown on glycerol plus lactate (Fig. 4) and glucose (data not shown). *ENO1* genes containing deletions extending from position −767 to position −442 and beyond to position −212 were not expressed at detectable levels (Fig. 4). These data mapped the apparent 5′ boundary of a positive regulatory region between positions −447 and −442. Interestingly, *ENO1* genes containing deletions extending from position −767 to position −182 and beyond to position −121 were expressed at near wild-type levels in cells grown on glycerol plus lactate (Fig. 4). We presume that deletion of these latter sequences allows a putative positive regulatory element located upstream from the *Xba*I site at position −767 to activate *ENO1* expression. Evidence is presented below that the 5′ boundary of a negative regulatory region is located between positions −121 and −182. Deletions extending to

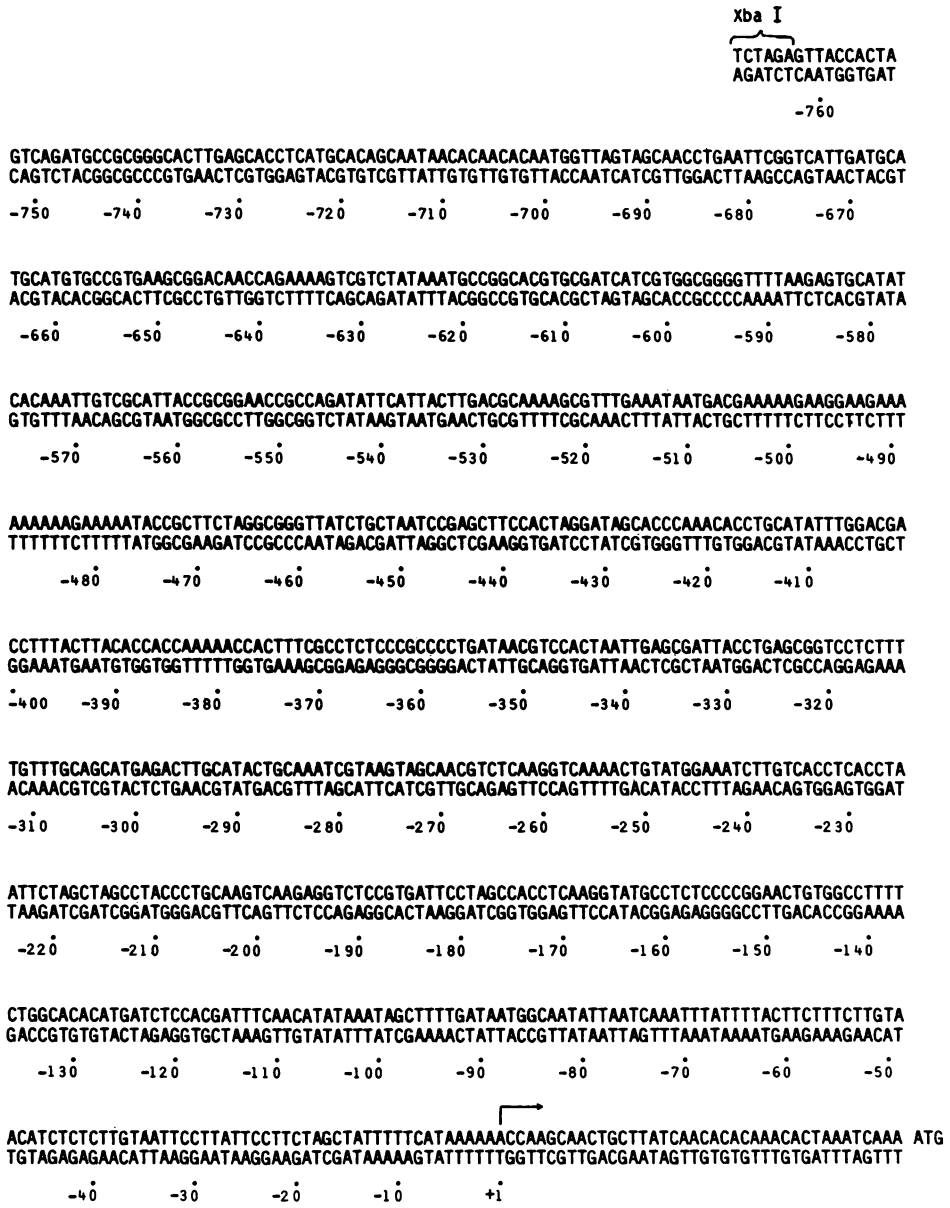

FIG. 2. Nucleotide sequence of the *ENO1* 5′-flanking region. The nucleotide sequence of the *ENO1* 5′-flanking region extending from the *Xba*I cleavage site 767 bp upstream from the transcription initiation site to the translation initiation codon was determined on both strands by the method of Maxam and Gilbert (8). The nucleotide sequence is numbered from the first nucleotide of the transcript synthesized in vivo from the *ENO1* gene (arrow) 40 bp upstream from the translation initiation codon.

position −100 and beyond were not expressed at detectable levels, suggesting that the TATAAA box located immediately upstream from position −100 is required for *ENO1* expression.

The apparent 3′ boundaries of these *cis*-acting regulatory regions were mapped by analyzing the expression of the *ENO1* gene containing deletion and insertion mutations extending from position −121 variable distances toward the *Xba*I site at position −767. The coordinates of these mutations are shown in Fig. 3, and Western blots for representative mutants are illustrated in Fig. 5. An *ENO1* gene containing a deletion extending from position −121 to position −126 was expressed at the same level as the wild-type gene in cells grown on glucose or glycerol plus lactate. *ENO1* genes containing deletion mutations extending from position −121 to positions −166 and −195 were expressed normally in cells grown on glycerol plus lactate; however, they were expressed at elevated levels in cells grown on glucose. These data mapped the apparent 3′ boundary of the negative regulatory region between positions −126 and −166. The data also suggest that this negative regulatory region interferes with glucose-dependent induction of *ENO1*. *ENO1* genes containing deletions extending from position −121 to positions −276, −415, and −440 were expressed normally in cells grown in glycerol plus lactate and at only slightly elevated levels in cells grown on glucose. Deletion of sequences between positions −121 and −489 abolished expression of the gene. These data mapped the apparent 3′ boundary of a positive regulatory region between positions −440 and −489.

Fine-structure deletion mapping of the positive and negative regulatory regions within the 5′-flanking sequences of *ENO1*. A series of small deletion and insertion mutations within the positive regulatory region were constructed and analyzed. The coordinates of these deletion mutations are diagrammed in Fig. 3, and representative Western blots are shown in Fig. 6. As expected, *ENO1* genes containing deletions extending from position −489 to position −442 or −369 were not expressed at detectable levels in cells grown on glucose or glycerol plus lactate. Genes containing deletions extending from position −489 to position −475 or −447 were expressed at wild-type levels in cells grown on either carbon source. These data are consistent with those shown in Fig. 4 and demonstrate that sequences located downstream from position −447 are sufficient for *ENO1* expression. *ENO1* genes containing deletions extending from position −440 to position −369 or −212 were expressed at low levels, while a gene containing a deletion extending from position −440 to position −182 was expressed at wild-type levels in cells grown on either carbon source. Since the apparent 5′ boundary of the negative regulatory element mapped between positions −212 and −182, these data suggest that sequences upstream from position −440 cannot activate expression of *ENO1*

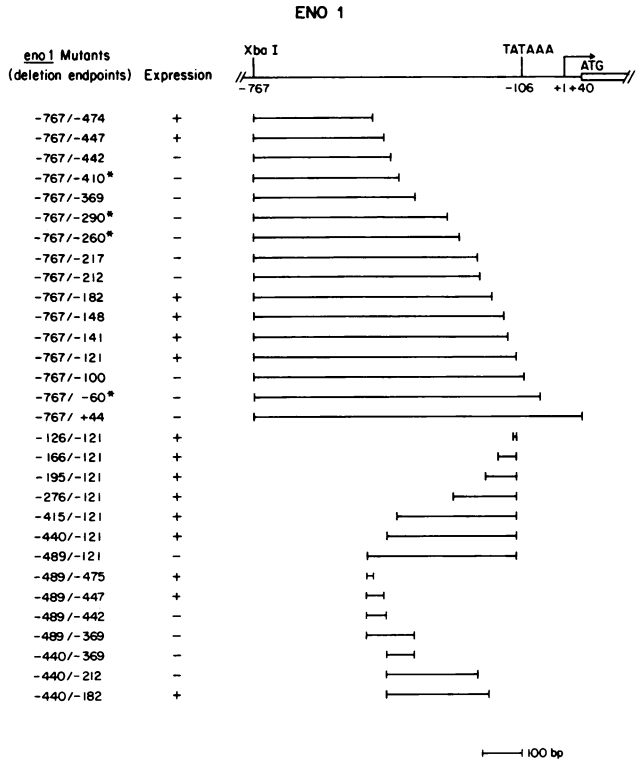

FIG. 3. Deletion and *Sal*I insertion mutations within the 5′-flanking region of *ENO1*. The solid line represents the *ENO1* 5′-flanking region. The bars below show the extent of each deletion. Each mutation contains a *Sal*I linker between the deletion endpoints. The coordinates of the deletion endpoints are numbered relative to the last *ENO1* nucleotide remaining at each endpoint and are shown at the left of the figure. Asterisks indicate endpoints which were not determined by DNA sequencing. Expression of each mutant *ENO1* gene was monitored by Western blotting analysis of transformant strains as described in Materials and Methods. Symbols: +, expression in cells grown on glucose or glycerol plus lactate; −, no detectable expression in cells grown on glucose or glycerol plus lactate.

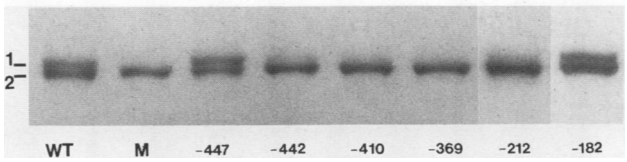

FIG. 4. Mapping the 5′ boundary of *cis*-acting sequences required for expression of the *ENO1* gene. Plasmids containing deletions within the 5′-flanking region of the *ENO1* gene extending from position −767 variable distances toward the translation initiation codon were integrated at the *ENO1* locus of strain S173-LA. Expression of each mutant *ENO1* gene was analyzed by Western blotting of whole-cell extracts obtained from log-phase cells grown on glycerol plus lactate as described in Materials and Methods. The deletion mutations extended from position −767 to the position indicated below each lane. Extracts obtained from strain S173-6B (WT) and strain S173-LA (M) were analyzed as controls. The positions of the enolase 1 and enolase 2 polypeptides are indicated.

unless the negative regulatory sequences are removed. As described earlier (Fig. 4), *ENO1* genes containing deletions extending from position −182 to −767 were expressed, and the expression was presumed to be dependent on sequences located upstream from position −767. *ENO1* genes containing deletions extending from position −182 to −489, however, were not expressed at detectable levels (Fig. 5). Based on these data and those shown in Fig. 6, we suggest that sequences immediately upstream from position −440 can activate transcription of the *ENO1* gene in the absence of the negative regulatory region.

To further define the negative regulatory region within the 5′-flanking sequences of *ENO1*, a series of small deletion and insertion mutations were constructed between positions −276 and −121. The coordinates of these deletion mutations are illustrated in Fig. 7. None of the mutations affected expression of *ENO1* in cells grown on glycerol plus lactate. However, the mutations defined sequences which interfered with glucose-dependent induction of *ENO1* expression. Removal of sequences between positions −143 and −121 had no effect on *ENO1* expression in cells grown on glucose. In contrast, deletions which removed all or a portion of the sequences between positions −178 and −143 resulted in an average 10-fold increase in expression of *ENO1* relative to the wild-type gene in cells grown on glucose. *ENO1* genes

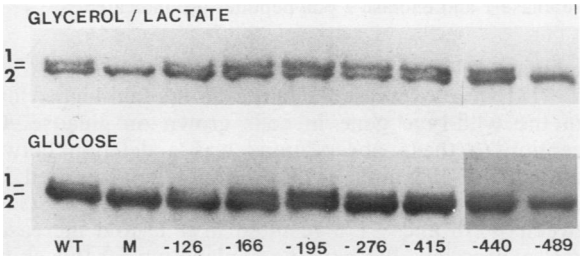

FIG. 5. Mapping the 3′ boundaries of *cis*-acting sequences required for expression of the *ENO1* gene. Plasmids containing deletions within the 5′-flanking region of the *ENO1* gene extending from position −121 variable distances toward position −767 were integrated at the *ENO1* locus of strain S173-LA. Expression of each mutant *ENO1* gene was analyzed by Western blotting of whole-cell extracts obtained from log-phase cells grown on glycerol plus lactate or glucose. The deletion mutations extended from position −121 to the position indicated below each lane. Extracts from strain S173-6B (WT) and strain S173-LA (M) were used as controls. The positions of the enolase 1 and enolase 2 polypeptides are indicated.

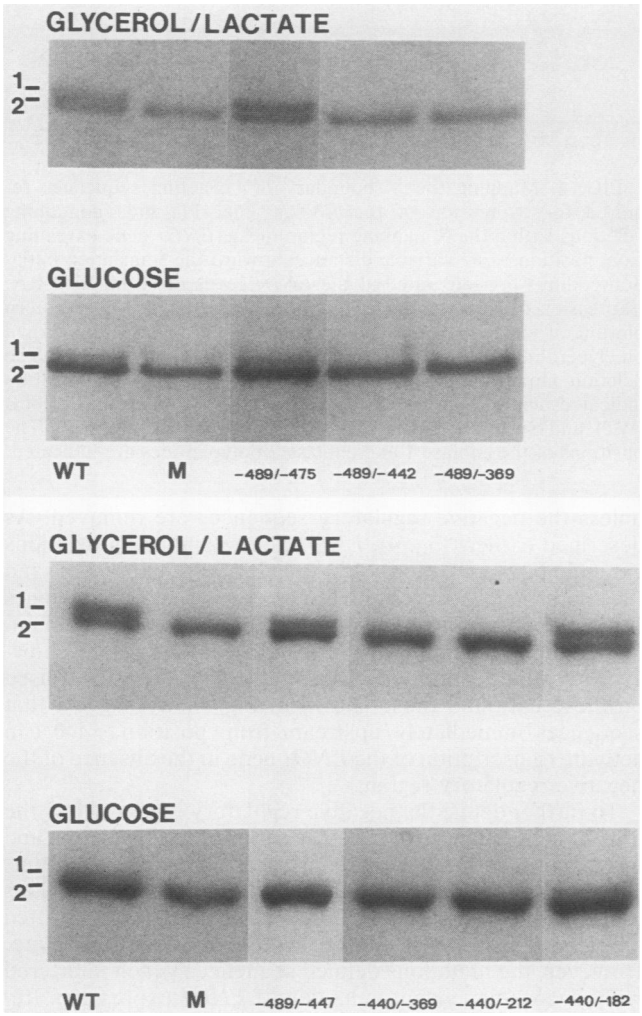

FIG. 6. Expression of the *ENO1* genes containing mutations within the UASs. Plasmids containing deletions within the upstream regulatory region were integrated at the *ENO1* locus of strain S173-LA. Expression of each mutant gene was monitored in log-phase cells grown on glycerol plus lactate or glucose after Western blotting of whole-cell extracts. The endpoints of each deletion mutation are indicated below each lane. Extracts from strain S173-6B (WT) and S173-LA (M) served as controls. The positions of the enolase 1 and enolase 2 polypeptides are indicated.

containing deletions of sequences between positions −276 and −181 were expressed at three- to fivefold higher levels than the wild-type gene in cells grown on glucose. One exception to these observations was a deletion between coordinates −195 and −173. This deletion resulted in a 5-fold increase in *ENO1* expression, whereas a deletion between −178 and −173 resulted in a 13-fold increase in *ENO1* expression. We have no explanation for this anomalous observation. The results summarized in Fig. 7 are consistent with those shown in Fig. 4 and 5 and defined a negative regulatory region located between positions −181 and −143.

To determine whether the positive and negative regulatory regions within the 5′-flanking sequences of *ENO1* regulate transcription of the gene, Northern blotting analysis was carried out on total cellular RNA isolated from strains carrying representative deletion and insertion mutations in *ENO1*. A hybridization probe complementary to the 3′ untranslated portion of *ENO1* mRNA was used for this analysis. Northern blots of representative mutants are shown in Fig. 8. The steady-state concentration of *ENO1* mRNA in strains carrying deletion mutations with coordinates −489 to −447 and −440 to −182 was indistinguishable from that in the wild type. Strains carrying deletion and insertion mutations with coordinates −489 to −442, −440 to −369, and −440 to −212 contained undetectable levels of *ENO1* mRNA. Finally, a strain carrying the −195 to −121 deletion mutation contained more than fivefold-higher concentration of *ENO1* mRNA than the wild-type parental strain when cells were grown in a medium containing glucose. All of these data were consistent with the Western blotting data shown in Fig. 5 and 6, indicating that the positive and negative *cis*-acting regulatory sequences modulate transcription of the *ENO1* gene.

Comparison of the functional properties of the upstream regulatory regions of *ENO1* and *ENO2*. The functional properties of the upstream regulatory sequences within the 5′-flanking sequences of *ENO1* and *ENO2* were compared by monitoring expression of heterologous gene fusions containing the upstream regulatory region from one enolase gene fused to the promoter region of the second enolase gene. The locations of the upstream activation sequences (UASs) and upstream repression sequences (URSs) in *ENO1* and *ENO2* are illustrated in Fig. 9. The presence of more than one UAS element in *ENO1* was inferred from the deletion mapping described above.

In the first series of experiments, a tribrid gene fusion was constructed. This gene fusion contained *ENO1* 5′-flanking sequences extending from an *Xba*I cleavage site at position −767 variable distances toward position −126. These *ENO1* sequences were ligated at a position 229 bp upstream from the *ENO2* transcriptional initiation site to generate an *ENO1-ENO2* hybrid 5′-flanking sequence. This hybrid 5′-flanking region was then ligated to the *ENO1* coding sequences and 3′-flanking sequences at a homologous *Hin*dIII site at codon 45 in the *ENO1* coding sequences. These tribrid gene fusions encoded the enolase 1 polypeptide. Expression of these genes was monitored by Western blotting analysis of whole-cell extracts prepared from transformants carrying the tribrid gene fusion integrated at the *ENO1* locus of the *ENO1* recipient strain. As illustrated in Fig. 10, tribrid genes containing *ENO1* 5′-flanking sequences extending from position −767 to position −440 and beyond to position −126 directed the synthesis of enolase 1 polypeptide at the same level as the endogenous *ENO2* gene when cells were grown in a medium containing glycerol plus lactate as the carbon source. A gene which contained *ENO1* 5′-flanking sequences extending from position −767 to position −489 did not direct the synthesis of detectable enolase 1 when cells were grown on glycerol plus lactate or on glucose. This latter gene lacked the *ENO1* upstream activation and repression sequences. Tribrid genes containing *ENO1* sequences extending from −767 to positions −415, −276, and −195 directed the synthesis of enolase 1 at levels comparable to the endogenous enolase 2 polypeptide when cells were grown in the presence of glucose. These genes lacked the upstream repression sequences located at position −162. A gene containing *ENO1* sequences extending from position −767 to position −126 directed the synthesis of enolase 1 at levels comparable to the wild-type *ENO1* gene. This gene contained the upstream repression sequences. Expression of the tribrid gene fusions (Fig. 10) was qualitatively and quantitatively similar to that of the *ENO1* gene deletions described in Fig. 3. These data demonstrated that *ENO1* sequences

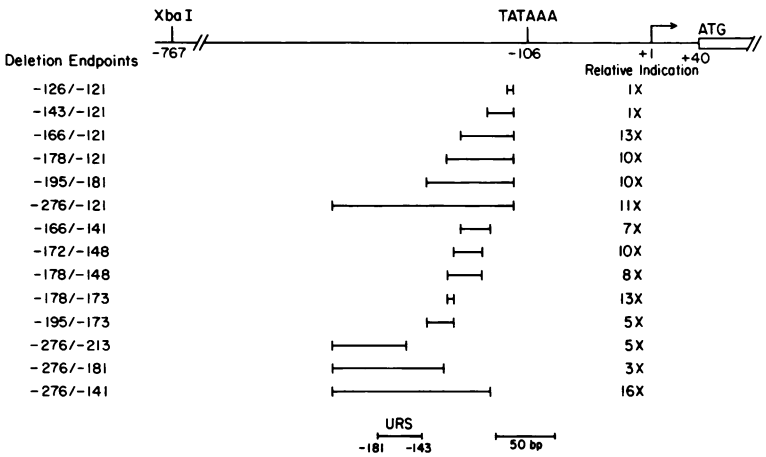

FIG. 7. Deletion mapping of the URSs in the *ENO1* gene. The line at the top represents the *ENO1* 5'-flanking region. The bars below indicate the extent of each deletion. Each mutant contains a *Sal*I linker between the deletion endpoints. The coordinates of the deletion endpoints are numbered relative to the last *ENO1* nucleotide remaining at each endpoint and are shown on the left. Expression of each mutant gene was monitored in cells grown on glucose by Western blotting analysis. The amounts of enolase 1 and enolase 2 were quantified as described in Materials and Methods; 1× indicates wild-type levels of expression of the *ENO1* gene in cells grown on glucose.

located upstream from position −126 were sufficient to confer accurate transcriptional regulation on the heterologous *ENO2* promoter sequences.

A second series of gene fusions were constructed which contained *ENO2* 5'-flanking sequences extending from an *Xba*I site located at position −1300 variable distances toward position −190. These *ENO2* sequences were ligated at a position 121 bp upstream from the *ENO1* transcription initiation site. Fused genes containing *ENO2* 5'-flanking sequences extending from position −1300 to positions −351 and −190 directed the synthesis of enolase 1 polypeptide at levels comparable to the endogenous enolase 2 polypeptide when cells were grown on a medium containing either glycerol plus lactate or glucose as the carbon source (Fig. 10). A gene containing *ENO2* 5'-flanking sequences extending to position −479 failed to direct the synthesis of detectable enolase 1 polypeptide when cells were grown on either carbon source (Fig. 10). This latter gene lacked both of the *ENO2* UASs. These results confirm that the *ENO2* UASs are sufficient to confer accurate transcriptional regulation on the heterologous *ENO1* promoter.

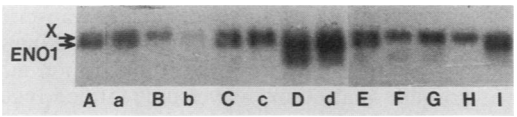

FIG. 8. Northern blot analysis of strains carrying deletion mutations within the 5'-flanking sequences of the *ENO1* structural gene. Northern blotting was performed with 5-μg samples of total cellular RNA isolated from log-phase wild-type and mutant strains grown in a medium containing glycerol plus lactate or glucose. A hybridization probe complementary to the 3' untranslated portion of *ENO1* mRNA was used. The position of the *ENO1* mRNA is indicated. A second, nonenolase mRNA which also hybridized with the probe was used as an internal control (band X). Uppercase letters indicate RNAs isolated from strains grown on glycerol plus lactate; lowercase letters indicate RNAs isolated from strains grown on glucose. Lanes: A and a, strain S173-6B; B and b, strain S173-LA; C and c, mutant (−126/−121); D and d, mutant (−195/−121); E, mutant (−489/−447); F, mutant (−489/−442); G, mutant (−440/−369); H, mutant (−440/−212); I, mutant (−440/−182).

DISCUSSION

The deletion mapping studies described in this report established the location of positive and negative regulatory regions within the 5'-flanking sequences of the *ENO1* structural gene. The positive regulatory region appeared to be complex. A functional UAS was located immediately downstream from a position 447 bp upstream from the transcription initiation site. Our results further suggest that UAS regions located immediately upstream from position −440 and upstream from position −767 can activate transcription of the *ENO1* gene but only in the absence of URS located approximately 162 bp upstream from the transcription initiation site. Multiple UASs were also identified within the 5'-flanking sequences of *ENO2* (2).

The surprising observation regarding the regulation of expression of the *ENO1* gene was the presence of a URS. Deletion of this URS region permitted glucose-dependent induction of *ENO1* which was quantitatively similar to that of the glucose-inducible *ENO2* gene. The URS therefore appears to be the crucial regulatory element for maintaining constitutive expression of the *ENO1* gene in cells grown on gluconeogenic or glycolytic carbon sources. The relative spacing between URS sequences and the UAS region or the TATAAA box in *ENO1* could be varied without significantly affecting URS function. Furthermore, the URS sequence contained within a segment of DNA which included the *ENO1* UAS region functioned normally when placed up-

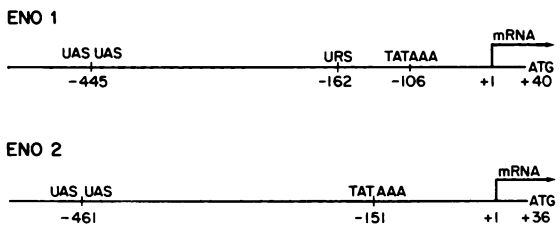

FIG. 9. *cis*-Acting regulatory regions of the *ENO1* and *ENO2* genes. Locations of the *cis*-acting regulatory regions within the 5'-flanking region of *ENO1* were deduced as described in Results. The locations of the *cis*-acting regulatory sequences in *ENO2* were determined previously (2).

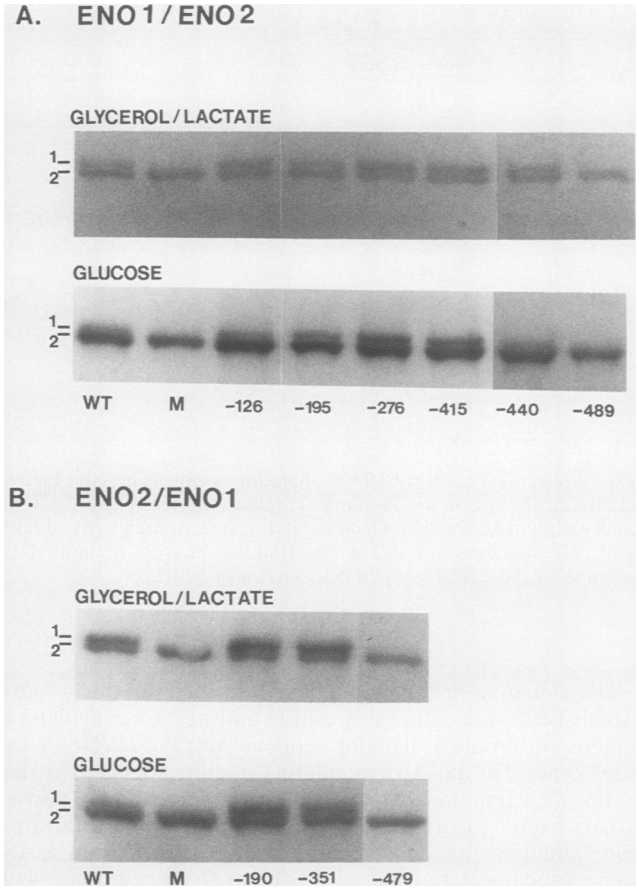

FIG. 10. Expression of enolase genes containing hybrid 5'-flanking sequences. Hybrid 5'-flanking regions were constructed as described in Materials and Methods by fusing the upstream regulatory region of one enolase gene at a site upstream from the TATAAA box in the other enolase gene. (A) *ENO1-ENO2* gene fusions contained *ENO1* sequences extending from an *Xba*I site at position −767 to the positions indicated below each Western blot joined at a site 229 bp upstream from the *ENO2* transcription initiation site. This hybrid 5'-flanking region was ligated to the *ENO1* coding sequences to generate a tribrid gene which encoded the enolase 1 polypeptide. (B) *ENO2-ENO1* gene fusions contained *ENO2* sequences extending from an *Xba*I site at position −1300 to the positions indicated below each Western blot joined at a site 121 bp upstream from the *ENO1* transcription initiation site. Western blotting was carried out with extract prepared from yeast transformants, grown in a medium containing the indicated carbon source, carrying each hybrid enolase gene. Extracts from strain S173-6B (WT) and strain S173-LA (M) were used as controls. The positions of the enolase 1 and enolase 2 polypeptides are indicated.

stream from the *ENO2* TATAAA box (Fig. 10). We did not observe a strict spacing requirement between the *ENO1* UASs and the TATAAA box; however, we did observe diminished glucose-dependent induction of gene expression when these activation sequences were brought within approximately 200 bp of the *ENO1* TATAAA sequence (Fig. 5) or the *ENO2* TATAAA sequence (Fig. 10). A similar spacing effect was observed for the *ENO2* gene (2).

The ability of the URS to regulate gene expression appears to be highly dependent on the nature of the UASs. Deletion of URS alone permitted glucose-dependent induction of *ENO1* expression but had no effect on gene expression in cells grown on glycerol plus lactate as the carbon source. In contrast, *ENO1* genes carrying deletions which removed sequences located downstream from position −440 were not expressed at detectable levels in cells grown on glycerol plus lactate or glucose unless the URS was also deleted. We have obtained preliminary evidence that insertion of the *ENO1* URSs between the complete UAS region of *ENO2* and its TATAAA box has no effect on expression of the *ENO2* gene in cells grown on glucose or glycerol plus lactate. Taken together, these data suggest that the URS interferes with the ability of the UAS regions to activate gene expression and that the extent of this URS effect is dependent on the nature of the UASs.

Negative regulatory sequences have been described within the 5'-flanking sequences of the yeast *MATα1* (12), *CAR1* (13), *CYC7* (14), and *STE6* (7) genes. In *MATα1* and *CAR1*, the URSs are located between the UAS region and the TATAAA box. In the *CAR1* gene, a point mutation within the putative URS leads to constitutive expression of the gene (13). Interestingly, *CAR1* sequences surrounding the site of this point mutation have significant nucleotide sequence homology with the core URSs from *ENO1*. It is therefore possible that putative *trans*-acting regulators of the *ENO1* URS also mediate repression of other yeast structural genes. Such a role has already been established for the *MATα2* gene product, which coordinately represses expression of yeast **a**-specific genes (7).

Analysis of expression of enolase genes containing hybrid 5'-flanking regions (Fig. 10) confirmed that the *ENO1* UASs and URS were sufficient to confer *ENO1*-like transcriptional regulation on the *ENO2* promoter. These studies also showed that the UASs of *ENO1* and *ENO2* are functionally similar. The observation that the upstream regulatory regions from either gene directed quantitatively similar levels of gene expression regardless of which enolase promoter region was used further suggests that the two enolase promoter regions, extending from sites upstream from the respective TATAAA boxes to the translation initiation codons, are functionally similar. We compared the nucleotide sequences of the *ENO1* and *ENO2* UASs. There were some short (6 to 8 bp) homologies among the sequences; however, additional studies will be necessary before functional significance can be assigned to these observations. It is tempting to speculate that sequences which are involved in coordinate regulation of expression of the two enolase genes are located within these UASs, since these regulatory sequences are required for expression of each enolase gene and because these regulatory sequences are functionally similar. Additional experiments will be necessary to confirm this point.

The results described in this report define transcriptional regulatory sequences within the *ENO1* 5'-flanking region extending 767 bp upstream from the transcription initiation site. It is possible that other, as yet unidentified regulatory sequences reside further upstream from the gene. We did observe expression of the *ENO1* gene when sequences extending from position −767 to position −182 and beyond to position −121 were deleted from the 5'-flanking region (Fig. 3 and 4). These observations suggest that there is another UAS region located upstream from position −767. Our results do not unequivocally distinguish between the fortuitous action of a UAS region from another gene and a second *ENO1* UAS region. It should be pointed out, however, that small deletions which removed the UAS sequences between positions −478 and −442 and beyond abolished transcription of the *ENO1* gene. This observation suggests that the observed expression of genes carrying large deletions extending from position −767 may be fortuitous.

ACKNOWLEDGMENTS

We thank Corey Levinson, Cetus Corporation, for providing us with oligonucleotide primers for determining the nucleotide sequence of deletion mutations.

R.C. was the recipient of a fellowship from Fundacion Gran Mariscal De Ayacucho, Caracao, Venezuela. A.E.P. is a predoctoral trainee on Genetics Training Grant GM-07467. This research was supported by Public Health Service grant GM-30307 from the National Institutes of Health and a grant from the March of Dimes Birth Defects Foundation.

LITERATURE CITED

1. **Clifton, D., S. B. Weinstock, and D. G. Fraenkel.** 1978. Glycolysis mutants in *Saccharomyces cerevisiae*. Genetics **88:** 1–11.
2. **Cohen, R., J. P. Hollan, T. Yokoi, and M. J. Holland.** 1986. Identification of a regulatory region that mediates glucose-dependent induction of the yeast enolase gene *ENO2*. Mol. Cell. Biol. **6:**2287–2297.
3. **Holland, M. J., J. P. Holland, G. P. Thill, and K. A. Jackson.** 1981. The primary structures of two yeast enolase genes. J. Biol. Chem. **256:**1385–1395.
4. **Holland, M. J., T. Yokoi, J. P. Holland, K. Myambo, and M. A. Innis.** 1987. The *GCR1* gene encodes a positive transcriptional regulator of the enolase and glyceraldehyde-3-phosphate dehydrogenase gene families in *Saccharomyces cerevisiae*. Mol. Cell. Biol. **7:**813–820.
5. **Howe, J. G., and J. W. B. Hershey.** 1981. A sensitive immunoblotting method for measuring protein synthesis initiation factor levels in lysates of *Escherichia coli*. J. Biol. Chem. **256:** 12836–12839.
6. **Ito, H., Y. Fukuda, K. Murata, and A. Kimura.** 1983. Transformation of intact yeast cells treated with alkali cations. J. Bacteriol. **153:**163–168.
7. **Johnson, A. D., and I. Herskowitz.** 1985. A repressor (*MAT*α2 product) and its operator control expression of a set of cell type specific genes in yeast. Cell **42:**237–247.
8. **Maxam, A., and W. Gilbert.** 1980. Sequencing end-labeled DNA with base-specific chemical cleavages. Methods Enzymol. **65:**499–560.
9. **McAlister, L., and M. J. Holland.** 1982. Targeted deletion of a yeast enolase structural gene. J. Biol. Chem. **257:**7181–7188.
10. **McKnight, S. L., and R. Kingsbury.** 1982. Transcriptional control signals of a eukaryotic protein-coding gene. Science **217:**316–324.
11. **Sanger, F., S. Nicklen, and A. R. Coulson.** 1977. DNA sequencing with chain-terminating inhibitors. Proc. Natl. Acad. Sci. USA **74:**5463–5467.
12. **Siliciano, P. G., and K. Tatchell.** 1984. Transcription and regulatory signals at the mating type locus in yeast. Cell **37:**969–978.
13. **Sumrada, R. A., and T. A. Cooper.** 1985. Target sites for positive and negative regulatory elements controlling expression of an inducible eucaryotic gene, p. 291–301. *In* R. Calendar and L. Gold (ed.), Sequence specificity in transcription and translation. Alan R. Liss, Inc., New York.
14. **Wright, C. F., and R. S. Zitomer.** 1984. A positive regulatory site and a negative regulatory site control the expression of the *Saccharomyces cerevisiae CYC7* gene. Mol. Cell. Biol. **4:**2023–2030.